Gadolinium in water Cherenkov detectors improves detection of supernova ν_e

Ranjan Laha[1,2,*] and John F. Beacom[1,2,3,†]

[1]*Center for Cosmology and AstroParticle Physics (CCAPP), Ohio State University,
Columbus, Ohio 43210, USA*
[2]*Department of Physics, Ohio State University, Columbus, Ohio 43210, USA*
[3]*Department of Astronomy, Ohio State University, Columbus, Ohio 43210, USA*
(Received 20 December 2013; published 17 March 2014)

Detecting supernova ν_e is essential for testing supernova and neutrino physics, but the yields are small and the backgrounds from other channels large, e.g., $\sim 10^2$ and $\sim 10^4$ events, respectively, in Super-Kamiokande. We develop a new way to isolate supernova ν_e, using gadolinium-loaded water Cherenkov detectors. The forward-peaked nature of $\nu_e + e^- \rightarrow \nu_e + e^-$ allows an angular cut that contains the majority of events. Even in a narrow cone, near-isotropic inverse beta events, $\bar{\nu}_e + p \rightarrow e^+ + n$, are a large background. With neutron detection by radiative capture on gadolinium, these background events can be individually identified with high efficiency. The remaining backgrounds are smaller and can be measured separately, so they can be statistically subtracted. Super-Kamiokande with gadolinium could measure the total and average energy of supernova ν_e with $\sim 20\%$ precision or better each (90% C.L.). Hyper-Kamiokande with gadolinium could improve this by a factor of ~ 5. This precision will allow powerful tests of supernova neutrino emission, neutrino mixing, and exotic physics. Unless very large liquid argon or liquid scintillator detectors are built, this is the only way to guarantee precise measurements of supernova ν_e.

I. INTRODUCTION

Supernovae are some of the most spectacular electromagnetic displays in the Universe. Understanding them is essential for many areas of physics and astrophysics. Core-collapse supernovae are massive stars ($\gtrsim 8M_\odot$) that, at the end of their burning cycles, collapse under gravity to form a neutron star or black hole [1–8]. These collapses are potential sites for gravitational-wave production [9–11], gamma-ray bursts [12], heavy-element nucleosynthesis [13,14], and cosmic-ray acceleration [15].

It is difficult to learn about the core properties and collapse mechanism using electromagnetic light curves, as the surface of last scattering of photons is in the outer envelope. Neutrinos, on the other hand, being weakly interacting, have their surface of last scattering much deeper inside, within the core. Neutrinos carry about $\sim 99\%$ of the binding energy released during the collapse of the star. Precise measurements of all flavors of neutrinos can provide much information about a supernova [16–34].

The only supernova neutrinos ever detected were from SN 1987A [35,36]. Even this modest data has been invaluable for understanding neutrinos and supernovae. Only $\bar{\nu}_e$ were detected, through the inverse beta channel, $\bar{\nu}_e + p \rightarrow e^+ + n$, leading to, e.g., constraints on the total and average energy in this flavor [37–40]. (We assume that the first event was not due to neutrino-electron elastic scattering, which has a very small probability.)

Computer simulations of supernova explosions have detailed predictions about the neutrino emission, but, due to the lack of a high-statistics Galactic supernova, it is not possible to adequately test these [41–49]. It is important to detect all flavors of neutrinos to measure the total and average energy in each. Because the differences between flavors may be modest, large numbers of events must be detected to ensure adequate precision.

Galactic supernovae occur only once every ~ 30 years. It is essential that a variety of detectors be ready to detect all flavors of neutrinos well to understand the physics and astrophysics of core-collapse supernovae. Using present detectors, it will be easy to measure supernova $\bar{\nu}_e$ and ν_x, via inverse beta and elastic scattering on protons, respectively [50–53]. Unless very large liquid argon [54,55] or liquid scintillator detectors [56,57] are built, or other techniques become experimentally viable [58–63], there will be no way to guarantee the clean detection of supernova ν_e in adequate numbers. The difficulties of measuring the ν_e spectrum well enough have long been known; e.g., see Refs. [64–72].

Here we show how this problem could be solved by using gadolinium (Gd) in Super-Kamiokande (Super-K) and other large water Cherenkov detectors. The addition of Gd to Super-K was proposed to improve the detection of $\bar{\nu}_e$. Ironically, this would also improve the detection of ν_e. We add new ideas to those briefly noted in Ref. [73] and perform the first detailed calculations, showing how supernova ν_e could be measured precisely.

---

*laha.1@osu.edu
†beacom.7@osu.edu

The principal technique is to use neutrino-electron scattering, $\nu_e + e^- \to \nu_e + e^-$. These events are forward peaked, so a narrow cone contains the majority of them. The largest background is from inverse beta events. The use of Gd to detect neutrons will help in individually detecting and removing these events with high efficiency. The spectrum of $\bar{\nu}_e$ will be measured precisely so that the remaining inverse beta and $\bar{\nu}_e + e^-$ scattering events can be statistically subtracted from the forward cone. Liquid scintillator detectors can detect ν_x ($= \nu_\mu + \nu_\tau$) well enough through $\nu + p \to \nu + p$ scattering, so the $\nu_x + e^-$ scattering events can be statistically subtracted.

In addition, we show how gadolinium will improve the prospects for measuring ν_e charged-current interactions with oxygen. This channel is only important if the average energy of ν_e is large, either intrinsically or due to efficient mixing with sufficiently hot ν_x. Recent supernova simulations suggest that none of the flavors has a large average energy, and that the differences between flavors are modest, so that these interactions with oxygen may not be important. In contrast, the neutrino-electron scattering events would be measured well in all scenarios if Gd is used to reduce backgrounds.

Detecting supernova ν_e will be helpful in constructing the initial spectrum of these neutrinos, testing neutrino mixing scenarios, and probing exotic physics. We concentrate on detecting the ν_e emitted during the full duration of the burst; however, this technique could also help in detecting the short neutronization burst ν_e in Mton water Cherenkov detectors [74].

The outline for this article is as follows. In Sec. II, we discuss the various theoretical and experimental inputs required to isolate supernova ν_e. In Sec. III, we discuss how this can constrain the ν_e spectrum parameters, and we conclude in Sec. IV.

II. CALCULATION INPUTS

We first discuss the neutrino spectra from a supernova, followed by the various detection channels in a water Cherenkov detector. We then outline the detection strategy that we propose to use to detect supernova ν_e in a water Cherenkov detector with gadolinium.

A. Supernova neutrino spectra

A supernova neutrino burst lasts for ~ 10 sec and includes all flavors of neutrinos. The total binding energy released in the explosion is $\sim 3 \times 10^{53}$ erg. We assume that the total energy is equipartitioned between the six species so that the total energy carried by each ν (or $\bar{\nu}$) flavor is $\sim 5 \times 10^{52}$ erg. The supernova is assumed to be at a distance of 10 kpc, the median distance of core collapse progenitor stars in our Galaxy, which is slightly farther than the distance to the Galactic center [75].

Supernova neutrinos are emitted in a quasithermal distribution. For concreteness, we take a particular modified Maxwell–Boltzmann spectrum [76,77],

$$f(E_\nu) = \frac{128}{3} \frac{E_\nu^3}{\langle E_\nu \rangle^4} \exp\left(-\frac{4E_\nu}{\langle E_\nu \rangle}\right), \qquad (1)$$

where this is normalized to unity. Using a regular Maxwell–Boltzmann or a Fermi–Dirac spectrum with the same average energy gives more neutrinos at high energies. For the electron-scattering and inverse-beta channels, the increased number of events is $\lesssim 5\%$. For the oxygen channel, which depends very sensitively on neutrino energy, the number of events can increase by $\sim 50\%$. Our choice of spectrum is conservative, and our results can only improve if other neutrino spectra are appropriate.

For the average energies of the initial spectra, we take $\langle E_{\nu_e} \rangle \approx 11$–12 MeV, $\langle E_{\bar{\nu}_e} \rangle \approx 14$–15 MeV, and $\langle E_{\nu_x} \rangle \approx 15$–18 MeV; the hierarchy follows from the different strengths of interaction in the supernova core. Neutrino mixing effects in the supernova [78–87] or on Earth [67,88,89] can have a dramatic effect on the final spectra, even exchanging them. Then the ν_e (or $\bar{\nu}_e$) spectrum could have an average energy of ~ 15–18 MeV, increasing the yields of charged-current detection channels. (The yields of neutral-current detection channels do not change for active-flavor mixing.) To tell how efficient the mixing is, we need to measure the ν_e detection spectra precisely.

A model independent neutrino signal from a supernova is the neutronization burst, which consists of a short pulse (~ 25 msec) of initially pure ν_e before the ~ 10 sec emission of neutrinos of all flavors [74]. Depending on the neutrino mixing scenario, the number of neutronization ν_e detected in a Mton water Cherenkov detector for a Galactic supernova is ~ 30–100 [74,90]. Our detection strategy will also be useful in this case. In Super-Kamiokande (fiducial volume 32 kton), the number of events due to neutronization ν_e is only $\sim \mathcal{O}(1)$.

B. Neutrino detection interactions

All flavors of neutrinos and antineutrinos can be detected with the $\nu + e^- \to \nu + e^-$ channel. The recoil kinetic energy of the scattered electron varies between 0 and $2E_\nu^2/(m_e + 2E_\nu)$. The forward-scattered electron makes an angle α with the incoming neutrino given by $\cos\alpha = \sqrt{T_e/(T_e + 2m_e)}(E_\nu + m_e)/E_\nu$, where T_e is the kinetic energy of the recoil electron.

The differential cross section for neutrino-electron elastic scattering is [91]

$$\frac{d\sigma}{dT_e} = \frac{G_F^2 m_e}{2\pi}\left[(g_V + g_A)^2 + (g_V - g_A)^2\left(1 - \frac{T_e}{E_\nu}\right)^2 \right.$$
$$\left. + (g_A^2 - g_V^2)\frac{m_e T_e}{E_\nu^2}\right], \qquad (2)$$

where G_F is the Fermi coupling constant; $g_V = 2 \sin^2\theta_W \pm 1/2$ for ν_e and ν_x, respectively; and $g_A = \pm 1/2$ for ν_e and ν_x, respectively. For antineutrinos, $g_A \to -g_A$. When integrated over T_e, the total cross section $\sigma(E_\nu) \propto m_e E_\nu$.

Only $\bar{\nu}_e$ were detected from SN 1987A, via the inverse beta reaction, $\bar{\nu}_e + p \to e^+ + n$, where p denotes free hydrogen (protons) in water and the positrons are emitted almost isotropically. The cross section for this process is $\sigma(E_\nu) \simeq 0.0952 \times 10^{-42}(E_\nu - 1.3)^2(1 - 7E_\nu/m_p)$ cm^2 where m_p is the proton mass, the energies are in MeV, the threshold of the reaction is $E_\nu > 1.8$ MeV, and $T_e \simeq E_\nu - 1.8$ MeV [50,51].

The neutron thermalizes by elastic collisions and is captured on protons as $n + p \to d + \gamma$ in about 200 μs. The emitted gamma ray has an energy of 2.2 MeV, which cannot be reliably detected in Super-K due to low-energy detector backgrounds [92]. To unambiguously detect the emitted neutron, it has been proposed to add Gd to large water Cherenkov detectors. Then the neutron will be thermalized and captured on Gd in about 20 μs, leading to 3–4 gamma rays with a total energy of about 8 MeV, which is easily detectable in Super-K [73].

Electron neutrinos can also be detected in water Cherenkov detectors by $\nu_e + {}^{16}\text{O} \to e^- + {}^{16}\text{F}^*$ [64], where most of the final-state decay products of the excited ${}^{16}\text{F}^*$ nucleus are not detectable. The threshold for this reaction is ≈ 15 MeV, and the electron kinetic energy is $T_e \approx E_\nu{-}15$ MeV. In the energy range 25 MeV $\le E_\nu \le$ 100 MeV, the cross section is given by $\sigma(E_\nu) \approx 4.7 \times 10^{-40}(E_\nu^{0.25}{-}15^{0.25})^6$ cm^2, for energies in MeV [64,93]. The angular distribution of the electrons is slightly backward tilted. The steep energy dependence of the cross section means that ν_e can only be detected well if the average energy is large, say, due to mixing.

We neglect other neutrino interactions with oxygen ($\bar{\nu}_e$ charged-current [64] and all-flavor neutral-current [94]), as they are not our focus and their yields are small compared to that from the inverse-beta channel.

The time-integrated flux for single neutrino flavor is

$$\frac{dF}{dE_\nu} = \frac{1}{4\pi d^2}\frac{E_\nu^{\text{tot}}}{\langle E_\nu \rangle} f(E_\nu), \qquad (3)$$

where E_ν^{tot} denotes the total energy in that ν flavor and d is the distance to the supernova. The observed event spectrum in the detector is

$$\frac{dN}{dT_e} = N_T \int_{E_{\min}}^{\infty} dE_\nu \frac{dF}{dE_\nu}(E_\nu)\frac{d\sigma}{dT_e}(E_\nu, T_e), \qquad (4)$$

where N_T is the appropriate number of targets. For a larger average energy, the thermally averaged cross section is larger, but the flux is smaller (because the total energy is taken to be fixed). For neutrino-electron scattering, these effects nearly cancel, making the total number of events

TABLE I. Expected numbers of events in Super-K for a Galactic supernova at a distance of 10 kpc for different values of the neutrino average energy (we do not round the numbers so that small differences remain visible). The total energy of the supernova is assumed to be 3×10^{53} erg, equipartitioned among all flavors (here $\nu_x = \nu_\mu + \nu_\tau$). The detection threshold during a burst is assumed to be $T_e = 3$ MeV. Other interactions with oxygen are neglected because their yields are small compared to that of inverse-beta decay.

Detection channel	12 MeV	15 MeV	18 MeV
$\nu_e + e^- \to \nu_e + e^-$	188	203	212
$\bar{\nu}_e + e^- \to \bar{\nu}_e + e^-$	56	64	70
$\nu_x + e^- \to \nu_x + e^-$	60	64	68
$\bar{\nu}_x + e^- \to \bar{\nu}_x + e^-$	48	54	56
$\nu_e + {}^{16}\text{O} \to e^- + {}^{16}\text{F}^*$	16	70	202
$\bar{\nu}_e + p \to e^+ + n$	5662	7071	8345

almost insensitive to the average energy. The shape of the electron recoil spectrum does change, which provides sensitivity to the average energy.

Table I shows the expected number of events in Super-K for these reactions under different assumptions about the neutrino average energy. For additional details about the detection of neutrinos from a Galactic supernova in water Cherenkov detectors, see the references already cited as well as Refs. [95–97].

C. Proposed detection strategy

We focus on Super-K, the largest detector with low intrinsic backgrounds [98]. We assume that supernova events can be detected in the full inner volume of 32 kton. Super-K measures the energy, position, and direction of charged particles with very high efficiency. During a burst, detector backgrounds can be ignored. There is extensive ongoing research on employing Gd in Super-K [73,99,100]. The efficiency of neutron capture on Gd will be known from calibration data.

We employ the $\nu_e + e^- \to \nu_e + e^-$ reaction to detect the ν_e and look for the forward-scattered electrons. Knowing the direction of the Galactic supernova, if we make an angular cut of half-angle 40° (appropriate for the lowest energy $\nu_e + e^-$ events [98]), then $\sim 68\%$ of the electron-scattering events will be in that cone. The forward-scattered electrons can also locate the supernova to within a few degrees [75,93,101,102].

Figure 1 shows the recoil spectra for neutrino-electron scattering for all flavors. (We use kinetic energy, but Super-Kamiokande conventionally uses the total energy, $E_e = T_e + m_e$.) Because the energy range is so broad, the effects of energy resolution smearing ($\sim 15\%$ near 10 MeV) were found to be modest and are not included. As can be seen from the figure, ν_e has the largest number of events. This is important, because the other flavors of neutrino-electron scattering events are an irreducible background to the $\nu_e + e^-$ events.
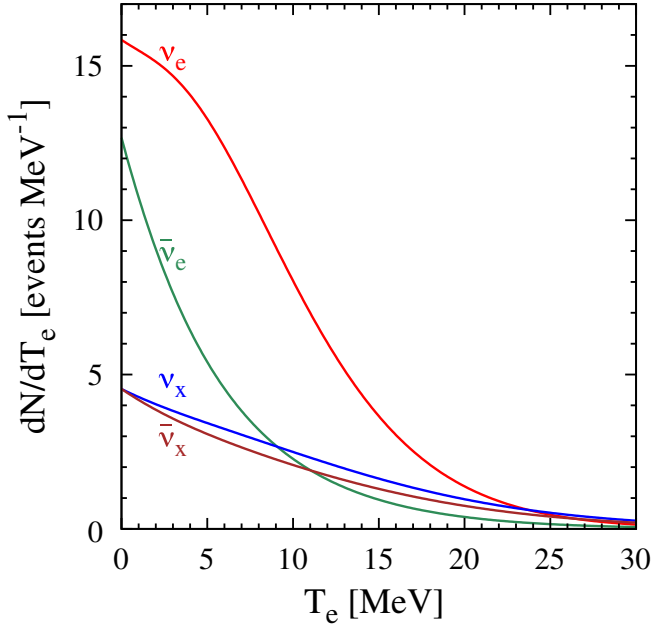
FIG. 1 (color online). Electron spectra for the $\nu + e^- \rightarrow \nu + e^-$ detection channels for a supernova in Super-K. These are just the events in the forward $40°$ cone ($\sim 68\%$ of the total). We take $\langle E_{\nu_e} \rangle = 12$ MeV, $\langle E_{\bar{\nu}_e} \rangle = 15$ MeV, and $\langle E_{\nu_x} \rangle = 18$ MeV; the other assumptions are listed in Table I.

The largest number of events will be due to the inverse beta reaction, which is almost isotropic. Neutron detection on Gd will individually identify $\sim 90\%$ of these events. The very large number of events will determine the $\bar{\nu}_e$ parameters precisely ($\sim 1\%$ with $\sim 10^4$ events), which will be used to statistically subtract the remaining inverse beta events. Events from other detection channels can also be statistically subtracted.

III. SUPERNOVA ν_e DETECTION AND CONSTRAINTS

We first discuss the typically assumed range of supernova neutrino spectrum parameters and show spectra for some representative neutrino mixing scenarios. We then calculate fits for the neutrino spectrum parameters and show the results for these and other cases.

A. Calculated detection spectra

Several cases can be considered for the initial spectra and how they are changed by neutrino mixing. Our focus is on testing the ν_e sector. We first note the two extreme cases that we want to differentiate and then mention some other possibilities. There are also cases intermediate between the extremes we note. We do not try to identify these cases in terms of active-flavor neutrino mixing scenarios, given the large uncertainties in the problem, especially in the initial neutrino spectra. Our focus on improving the measurements, and the interpretation in terms of supernova emission and neutrino mixing, will come once there is a detection.

Case A has $\langle E_{\nu_e} \rangle \approx 12$ MeV and $\langle E_{\nu_x} \rangle \approx 15–18$ MeV; i.e., there is a hierarchy of average energies between the flavors initially, and neutrino mixing *has not* interchanged them (other assumptions are as above).

Case B has $\langle E_{\nu_e} \rangle \approx 15–18$ MeV, and one flavor of ν_x has $\langle E_{\nu_x} \rangle \approx 12$ MeV (the other flavors of ν_x have $\langle E_{\nu_x} \rangle \approx 15–18$ MeV); i.e., there is a hierarchy of average energies between the flavors initially, and neutrino mixing *has* interchanged them.

If the average energy of ν_x were large and mixing were effective at exchanging the spectra of antineutrinos instead of neutrinos, this would be evident in the $\bar{\nu}_e + p$ spectrum; this is disfavored by the SN 1987A data. If all flavors had a low average energy, this would be evident in the $\bar{\nu}_e + p$ and $\nu + p$ spectra (because the $\nu + p$ channel is a neutral-current interaction, its yield is not changed by active-flavor mixing). The yields of these and other channels can decide everything except the differences between cases A and B. That's the open problem: What is the ν_e spectrum?

When the ν_e average energy is high, $\nu_e + {}^{16}O$ is a good detection channel; otherwise, it gives no useful signal because the yields are too small to be detected in the presence of backgrounds. Typical average energies from supernova simulations are markedly lower than the values assumed a decade or two ago, so $\nu_e + {}^{16}O$ is now a much less favorable channel. Besides $\nu_e + e^-$ in Super-K, there is no other detection channel in any existing detector that produces enough identifiable ν_e events when the average energy is low. The yield of $\nu_e + e^-$ barely changes with changes in the average energy. Another important change from a decade or two ago is that much lower energies can be detected, which improves the spectrum shape tests.

The main background for these reactions is the inverse-beta events. Some of these numerous events can be removed using an angular cut, but they still pose a formidable background. This is shown in the left panel in Fig. 2 for the same average energies as in Fig. 1. There are $\sim 128 \, \nu_e + e^-$ events in the $40°$ cone, but this is swamped by ~ 827 inverse-beta events. In the absence of neutron tagging, it will be difficult to extract the ν_e signal from this background.

However, adding Gd to Super-K has a dramatic effect. Assuming that the efficiency of neutron detection in a Gd-loaded Super-K is 90%, the inverse-beta background will decrease to 83 events. This strongly improves the detection prospects of ν_e. The $\bar{\nu}_e$ spectrum will be well measured by cleanly identified inverse-beta decay events using neutron detection by Gd. This will allow statistical subtraction of the backgrounds due to $\bar{\nu}_e + e^-$ and the remaining $\bar{\nu}_e + p$ events. Liquid scintillator detectors will measure the spectrum of ν_x from the $\nu + p$ channel, which is most sensitive to the flavors with the highest average energies. This will allow statistical subtraction of the backgrounds
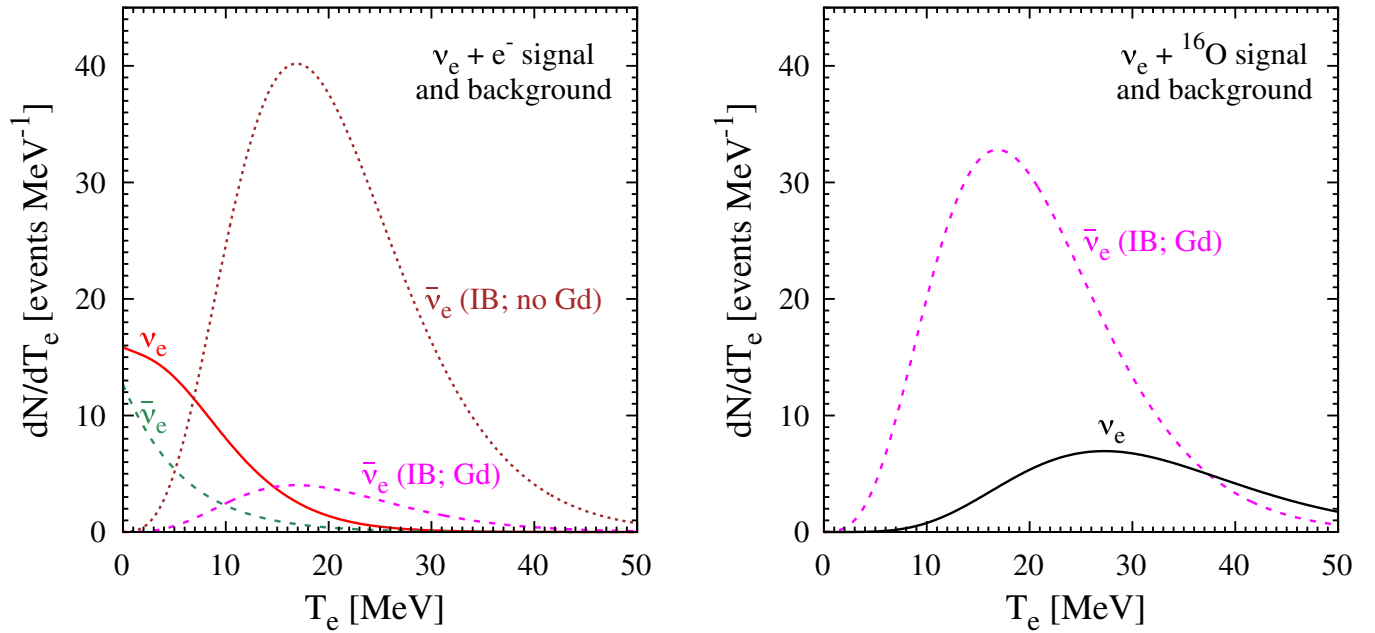
FIG. 2 (color online).   Detectable electron (or positron) spectra in Super-K without or with Gd. The two panels consider different cases for $\langle E_{\nu_e}\rangle$ after neutrino mixing. Other parameters, including $\langle E_{\bar{\nu}_e}\rangle = 15$ MeV, are as in Fig. 1. Left Panel: For case (A) with $\langle E_{\nu_e}\rangle = 12$ MeV, we focus on the $\nu_e + e^-$ signal (solid line) in the forward 40° cone. The dotted line shows the large inverse-beta background without Gd, and the dashed lines show the most important backgrounds with Gd. Right panel: For case (B) with $\langle E_{\nu_e}\rangle = 18$ MeV, we focus on the $\nu_e + {}^{16}$O signal (solid line) in the region complementary to the forward 25° cone (note the different angle). The inverse beta background without Gd is too large to show, and the dashed line shows this background with Gd. Here the signal and background are both due to the Galactic supernova.
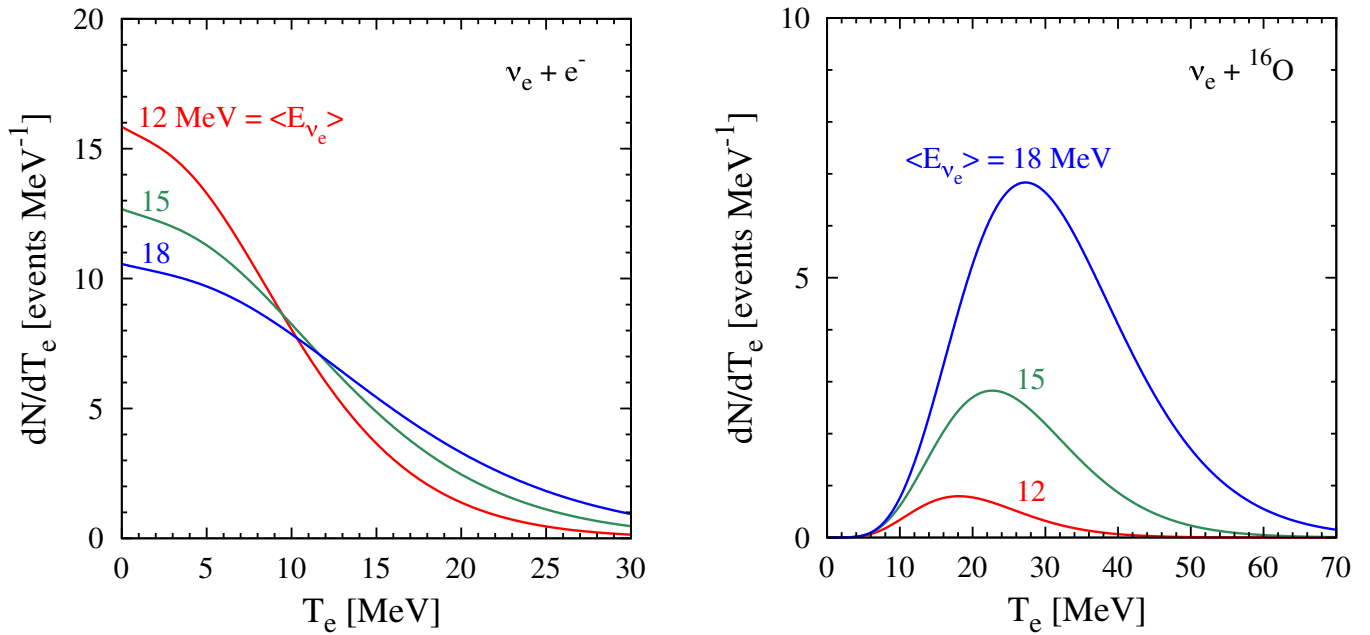

FIG. 3 (color online).   Detectable electron spectra in Super-K, ignoring backgrounds, for different assumed average energies for ν_e (12, 15, and 18 MeV) to show variants of the signals in Fig. 2. All spectra scale linearly with changes in the assumed total energy in ν_e. Other assumptions are as above. Note axis changes from Fig. 2. Left Panel: For the $\nu_e + e^-$ channel in the forward 40° cone. Right Panel: For the $\nu_e + {}^{16}$O channel in the region complementary to the forward 25° cone.

due to the $\nu_x + e^-$ channel. These subtractions only lead to modest increases in the uncertainties of the spectrum shown in the left panel of Fig. 2.

The $\nu_e + {}^{16}O$ channel is only useful if the ν_e average energy is large, as otherwise the yield is too small. Even for a ν_e average energy of 18 MeV, the backgrounds are still important. There are ~ 200 signal events in the whole detector. Excluding a forward cone of 25°, ~ 190 events remain. (The different choice of angle for the forward cone is because now we focus on higher energies, for which the angular resolution is better.) In a detector without Gd, these would be overwhelmed by the ~ 7071 inverse beta events, but neutron tagging by Gd will dramatically reduce this background. This situation is shown in the right panel in Fig. 2. Again assuming an efficiency of 90% in neutron tagging in a Gd-loaded Super-K, only ~ 707 of the inverse-beta events will remain. This enormous reduction in background will greatly help in isolating the $\nu_e + {}^{16}O$ signal.

Figure 3 shows how the detection spectra for $\nu_e + e^-$ and $\nu_e + {}^{16}O$ change with different assumptions about the ν_e average energy. The yield for $\nu_e + e^-$ elastic scattering depends only weakly on the average energy, but that for the $\nu_e + {}^{16}O$ reaction changes dramatically. See also Table I. Both channels also have characteristic spectrum changes as the average energy changes, as shown in Fig. 3.

B. Fits for neutrino spectrum parameters

The detection spectra in Fig. 2 show that adding Gd to Super-K will greatly reduce backgrounds for supernova ν_e. We quantify the improvement in the determination of the ν_e spectrum parameters, $\langle E_{\nu_e} \rangle$ and $E_{\nu_e}^{tot}$, by constructing a χ^2 and performing fits. We use

$$\chi^2 = \sum_i \left(\frac{\mathcal{O}_i(\langle E_{\nu_e}\rangle^0, E_{\nu_e}^{tot,0}) - T_i(\langle E_{\nu_e}\rangle, E_{\nu_e}^{tot})}{\sigma_i} \right)^2, \quad (5)$$

where $\mathcal{O}_i(\langle E_{\nu_e}\rangle^0, E_{\nu_e}^{tot,0})$ are the numbers of events in each bin assuming the fiducial values of the parameters, $T_i(\langle E_{\nu_e}\rangle, E_{\nu_e}^{tot})$ are the same allowing different values, and σ_i are the uncertainties on the fiducial numbers.

Because all spectra except ν_e will be well measured separately, here we only need to fit for the ν_e spectrum parameters. That is, we fit spectra like those in Fig. 3 after the remaining backgrounds shown in Fig. 2 have been statistically subtracted. In the χ^2 calculation, the numbers of events in the numerator are only those of the signals; the backgrounds affect the results by increasing the uncertainties in the denominator, which depend on the numbers of signal plus background events.

Put another way, if we set up a χ^2 for the data before the statistical subtractions (Fig. 2 instead Fig. 3), then the
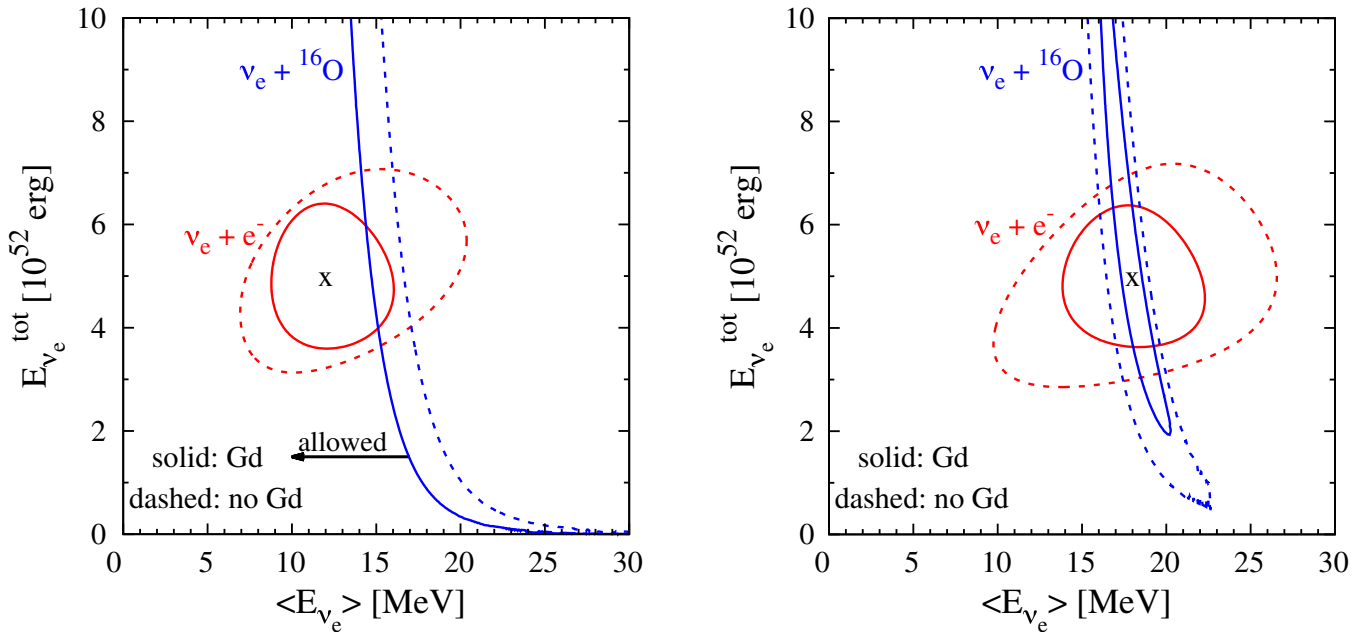

FIG. 4 (color online). Allowed regions (90% C.L. $\Delta\chi^2$ contours) for the ν_e spectrum parameters determined from the $\nu_e + e^-$ and $\nu_e + {}^{16}O$ channels separately. The combined constraints (not shown) closely follow what would be expected visually. The two panels are for different cases (fiducial parameters marked by an x), matching those of Fig. 2. Dashed lines indicate the contours when Gd is not used, and solid lines show the improvements when Gd is used. Left Panel: When the ν_e average energy is small, here 12 MeV, the $\nu_e + e^-$ channel gives a closed allowed region, but the $\nu_e + {}^{16}O$ channel only defines upper limits. Right Panel: When the ν_e average energy is large, here 18 MeV, both channels give closed allowed regions.
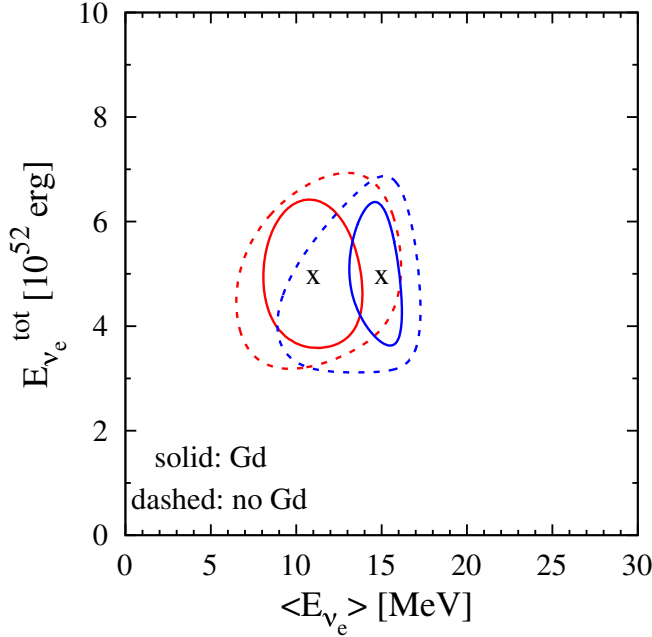
FIG. 5 (color online). Allowed regions (90% C.L. $\Delta\chi^2$ contours) for the ν_e spectrum parameters determined from the $\nu_e + e^-$ and $\nu_e + {}^{16}\mathrm{O}$ channels jointly. Two examples of fiducial parameters ($\langle E_{\nu_e}\rangle^0 = 11$ MeV and $\langle E_{\nu_e}\rangle^0 = 15$ MeV) are each marked with an x. The corresponding fit regions are shown without and with Gd.

contributions from flavors besides ν_e would cancel in the numerator but not the denominator. More precisely, those cancelations would occur only on average if typical statistical fluctuations were included.

To determine the allowed regions of parameters when a supernova is detected, we calculate $\Delta\chi^2$ relative to various assumed best-fit cases (using $\Delta\chi^2 = 4.6$ for two degrees of freedom to obtain the 90% C.L. regions).

Our results indicate the likely size and shape of the allowed regions once a supernova is detected. We make some reasonable approximations. The uncertainties on the initial spectra and the effects of neutrino mixing are large, and the uncertainties on the neutrino cross sections are moderate. In addition, we are considering only the time-averaged emission, whereas the average energies may vary during the burst. The widths of the bins were chosen to have approximately equal numbers of $\nu_e + e^-$ events in each bin (at least $\simeq 10$ events per bin). The numbers of events are then large enough that the Poisson uncertainties can be treated as Gaussian.

In case A from above, there is a hierarchy between the average energies of different flavors, but their spectra *are not* interchanged by mixing, so the average energy of ν_e is low. We take $\langle E_{\nu_e}\rangle^0 = 12$ MeV and $E_{\nu_e}^{\mathrm{tot},0} = 5 \times 10^{52}$ erg as fiducial parameters for this case.

If these are the true parameters of the supernova, then the left panel of Fig. 4 shows the likely precision with which the parameters would be reconstructed from the measured

data in Super-K without or with Gd. In this case, the primary constraint comes from the $\nu_e + e^-$ channel. The $\nu_e + {}^{16}\mathrm{O}$ channel does not have enough events relative to the backgrounds, though large values of $\langle E_{\nu_e}\rangle$ can be excluded by the nonobservation of a significant number of events. The presence of Gd reduces the size of the allowed region significantly. With both channels together, the allowed region would be centered on $\langle E_{\nu_e}\rangle = 12$ MeV and would range from roughly 9 to 14 MeV. Thus, with Gd, it would be possible to say that $\langle E_{\nu_e}\rangle$ is different from $\langle E_{\bar{\nu}_e}\rangle$ (which could be 15 MeV with $\sim 1\%$ precision). This would not be possible without Gd, so this is an important difference.

In case B from above, there is a hierarchy between the average energies of different flavors, and their spectra *are* interchanged by mixing, so the average energy of ν_e is high. We take $\langle E_{\nu_e}\rangle^0 = 18$ MeV and $E_{\nu_e}^{\mathrm{tot},0} = 5 \times 10^{52}$ erg as fiducial parameters for this case.

If these are the true parameters of the supernova, then the right panel of Fig. 4 shows the likely precision with which the parameters would be reconstructed from the measured data in Super-K without or with Gd. In this case, both channels have enough events to define allowed regions. The steep energy dependence of the $\nu_e + {}^{16}\mathrm{O}$ cross section gives a precise measurement of the average energy, though the large backgrounds and uncertainties mean that the total energy is not well determined. As before, the presence of Gd improves the precision, especially for the $\nu_e + e^-$ channel. With both channels together, the allowed region would be very small. It would be easy to distinguish case A and case B; Gd would greatly improve the significance of this comparison.

The presence of Gd is even more important when the neutrino average energies are closer to each other. This is seen in some simulations, e.g., Ref. [43], where $\langle E_{\nu_e}\rangle \approx 11$ MeV, and $\langle E_{\bar{\nu}_e}\rangle \approx \langle E_{\nu_x}\rangle \approx 15$ MeV. Because of the less pronounced hierarchy, it will be much harder to distinguish scenarios like case A and case B.

Figure 5 shows our results (joint constraints using both channels) for the allowed regions of the ν_e spectrum parameters. In this case, the presence of Gd does not completely separate the 90% C.L. contours, but it comes very close. Without Gd, the two allowed regions cannot be separated at all, which would significantly degrade the ability to test the physics.

Recent long-term simulations show that the average energy of the neutrinos can change during the ~ 10 sec emission time [23,103,104]. The average energy of ν_e typically changes from ~ 12 to ~ 6 MeV. For a detector like Super-Kamiokande, it might be difficult to detect this change of average energy. For a future detector like Hyper-Kamiokande, which will have better precision for the spectral paramaters (see later), such a difference could be distinguished.

IV. CONCLUSIONS

When the next Galactic supernova occurs, it is essential that we have a collection of detectors that can measure all neutrino flavors well. Without this, we will be unable to fully address many important questions. What is the total energy emitted in neutrinos, and how is it partitioned among flavors? Are the average energies of the various flavors different? What do these results say about neutrino mixing and tests of exotic physics? What do the differences between $\bar{\nu}_e$ and ν_e emission tell us about the neutron-to-proton ratio of the collapsing core?

At present, the only detector with a relatively large yield of ν_e events is Super-K. Even so, this is only $\sim 10^2$ events using the $\nu_e + e^-$ channel. If the average energy of ν_e is large enough, then the $\nu_e + {}^{16}\mathrm{O}$ channel will have a comparable number of events. The problem is the background of $\sim 10^4$ events from the inverse-beta channel, $\bar{\nu}_e + p$. This background can be reduced for $\nu_e + e^-$ using an angular cut, but not enough.

We demonstrate in detail a new technique to reduce backgrounds for both the $\nu_e + e^-$ and $\nu_e + {}^{16}\mathrm{O}$ channels. If Super-K adds Gd to improve the detection of $\bar{\nu}_e + p$, then $\sim 90\%$ of these events will be individually identified through detection of the neutron radiative capture on Gd in close time and space coincidence with the positron. This would dramatically reduce backgrounds for other channels. The remaining backgrounds can be statistically subtracted using independent measurements.

We show that the ν_e spectrum parameters, $\langle E_{\nu_e} \rangle$ (average energy) and $E_{\nu_e}^{\mathrm{tot}}$ (total energy), can be measured to $\sim 20\%$ or better if Super-K adds Gd. This is a significant improvement over the capabilities of Super-K without Gd. (For comparison, the precision for ν_x in existing scintillator detectors is comparable, and the precision for $\bar{\nu}_e$ in Super-K will be $\sim 1\%$.) Further, this improvement could be the difference between being able to answer essential questions or not. Unless very large liquid argon or liquid scintillator detectors are built, then we have no other way to adequately measure the ν_e spectrum.

Future extremely large water Cherenkov detectors like Hyper-Kamiokande would have a dramatic impact on detecting supernova ν_e using this technique. The ~ 25 times larger volume would reduce the uncertainty on the ν_e parameters by factor of $\sim \sqrt{25} = 5$. This requires using Gd in Hyper-Kamiokande, the prospects of which are prominently considered [105]. (This would also require a new very large liquid scintillator detector [56,57] for improved measurements of ν_x using the $\nu + p$ channel.)

This new method of determining supernova ν_e would help improve our understanding of supernovae and neutrinos in many ways. It provides yet another motivation for Super-K to add Gd. Given how infrequent Galactic supernovae are, it is essential that the opportunity to measure ν_e well not be missed.

[1] H. Janka and E. Mueller, Phys. Rep. **256**, 135 (1995).
[2] K. Langanke and G. Martinez-Pinedo, Rev. Mod. Phys. **75**, 819 (2003).
[3] A. Mezzacappa, Annu. Rev. Nucl. Part. Sci. **55**, 467 (2005).
[4] A. Burrows, L. Dessart, C. D. Ott, and E. Livne, Phys. Rep. **442**, 23 (2007).
[5] H.-T. Janka, K. Langanke, A. Marek, G. Martinez-Pinedo, and B. Mueller, Phys. Rep. **442**, 38 (2007).
[6] S. Woosley and T. Janka, arXiv:astro-ph/0601261.
[7] A. Burrows, Rev. Mod. Phys. **85**, 245 (2013).
[8] H.-T. Janka, Annu. Rev. Nucl. Part. Sci. **62**, 407 (2012).
[9] C. D. Ott, Classical Quantum Gravity **26**, 063001 (2009).
[10] K. Kotake, C.R. Phys. **14**, 318 (2013).
[11] S. Ando *et al.*, Rev. Mod. Phys. **85**, 1401 (2013).
[12] S. Woosley and J. Bloom, Annu. Rev. Astron. Phys. **44**, 507 (2006).
[13] F. Thielemann *et al.*, Prog. Part. Nucl. Phys. **46**, 5 (2001).
[14] S. Woosley and A. Heger, Phys. Rep. **442**, 269 (2007).
[15] P. Blasi, arXiv:1012.5005.
[16] T. A. Thompson, A. Burrows, and P. A. Pinto, Astrophys. J. **592**, 434 (2003).
[17] R. Tomàs, M. Kachelrieß, G. Raffelt, A. Dighe, H.-T Janka, and L. Scheck, J. Cosmol. Astropart. Phys. 09 (**2004**) 015.
[18] B. Dasgupta and A. Dighe, Phys. Rev. D **75**, 093002 (2007).
[19] A. Friedland and A. Gruzinov, arXiv:astro-ph/0607244.
[20] C. Lunardini, B. Muller, and H.-T. Janka, Phys. Rev. D **78**, 023016 (2008).
[21] Y. Suwa, T. Takiwaki, K. Kotake, and K. Sato, Astrophys. J. **690**, 913 (2009).
[22] A. Marek, H.-T. Janka, and E. Mueller, arXiv:0808.4136.
[23] L. Hudepohl, B. Muller, H.-T. Janka, A. Marek, and G. Raffelt, Phys. Rev. Lett. **104**, 251101 (2010).
[24] J. P. Kneller and C. Volpe, Phys. Rev. D **82**, 123004 (2010).

[25] E. Muller, H.-T. Janka, and A. Wongwathanarat, arXiv:1106.6301.

[26] M. D. Kistler, W. C. Haxton, and H. Yuksel, Astrophys. J. **778**, 81 (2013).

[27] T. Lund, A. Wongwathanarat, H.-T. Janka, E. Muller, and G. Raffelt, Phys. Rev. D **86** 105031 (2012).

[28] A. Wongwathanarat, H.-T. Janka, and E. Mueller, Astron. Astrophys. **552**, A126 (2013).

[29] K. Scholberg, Annu. Rev. Nucl. Part. Sci. **62**, 81 (2012).

[30] I. Tamborra, F. Hanke, B. Mueller, H.-T. Janka, and G. Raffelt, Phys. Rev. Lett. **111**, 121104 (2013).

[31] K. Nakamura, T. Takiwaki, K. Kotake, and N. Nishimura, arXiv:1207.5955.

[32] J. P. Kneller and A. W. Mauney, arXiv:1302.6601.

[33] J. P. Kneller and A. W. Mauney, Phys. Rev. D **88**, 025004 (2013).

[34] E. Borriello, S. Chakraborty, H.-T. Janka, E. Lisi, and A. Mirizzi, arXiv:1310.7488.

[35] K. Hirata et al. (KAMIOKANDE-II Collaboration), Phys. Rev. Lett. **58**, 1490 (1987).

[36] R. Bionta et al. (IMB Collaboration), Phys. Rev. Lett. **58**, 1494 (1987).

[37] B. Jegerlehner, F. Neubig, and G. Raffelt, Phys. Rev. D **54**, 1194 (1996).

[38] C. Lunardini and A. Y. Smirnov, Astropart. Phys. **21**, 703 (2004).

[39] H. Yuksel and J. F. Beacom, Phys. Rev. D **76**, 083007 (2007).

[40] G. Pagliaroli, F. Vissani, M. Costantini, and A. Ianni, Astropart. Phys. **31**, 163 (2009).

[41] B. Muller, H.-T. Janka, and H. Dimmelmeier, Astrophys. J. Suppl. Ser. **189**, 104 (2010).

[42] T. D. Brandt, A. Burrows, C. D. Ott, and E. Livne, Astrophys. J. **728**, 8 (2011).

[43] B. Mueller, H.-T. Janka, and A. Heger, Astrophys. J. **761**, 72 (2012).

[44] E. O'Connor and C. D. Ott, Astrophys. J. **762**, 126 (2013).

[45] K. Kotake, T. Takiwaki, Y. Suwa, W. I. Nakano, S. Kawagoe, Y. Masada, and S.-i. Fujimoto, Adv. Astron. **2012**, 428757 (2012).

[46] C. D. Ott, E. Abdikamalov, E. O'Connor, C. Reisswig, R. Haas, P. Kalmus, S. Drasco, A. Burrows, and E. Schnetter, Phys. Rev. D **86**, 024026 (2012).

[47] K. Kotake et al., PTEP **2012**, 01A301 (2012).

[48] B. Muller, H.-T. Janka, and A. Marek, Astrophys. J. **756**, 84 (2012).

[49] S. W. Bruenn, A. Mezzacappa, W. R. Hix, E. J. Lentz, O. E. Bronson Messer, E. J. Lingerfelt, J. M. Blondin, E. Endeve, P. Marronetti, and K. N. Yakunin, Astrophys. J. **767**, L6 (2013).

[50] P. Vogel and J. F. Beacom, Phys. Rev. D **60**, 053003 (1999).

[51] A. Strumia and F. Vissani, Phys. Lett. B **564**, 42 (2003).

[52] J. F. Beacom, W. M. Farr, and P. Vogel, Phys. Rev. D **66**, 033001 (2002).

[53] B. Dasgupta and J. F. Beacom, Phys. Rev. D **83**, 113006 (2011).

[54] R. Raghavan, Phys. Rev. D **34**, 2088 (1986).

[55] I. Gil Botella and A. Rubbia, J. Cosmol. Astropart. Phys. 08 (**2004**) 001.

[56] M. Wurm et al. (LENA Collaboration), Astropart. Phys. **35**, 685 (2012).

[57] Y.-F. Li, J. Cao, Y. Wang, and L. Zhan, Phys. Rev. D **88**, 013008 (2013).

[58] W. Haxton and C. W. Johnson, Nature (London) **333**, 325 (1988).

[59] G. M. Fuller, W. C. Haxton, and G. C. McLaughlin, Phys. Rev. D **59**, 085005 (1999).

[60] W. Haxton and R. Robertson, Phys. Rev. C **59**, 515 (1999).

[61] A. Ianni, D. Montanino, and F. Villante, Phys. Lett. B **627**, 38 (2005).

[62] R. Lazauskas, C. Lunardini, and C. Volpe, J. Cosmol. Astropart. Phys. 04 (**2009**) 029.

[63] T. Suzuki, A. Balantekin, and T. Kajino, Phys. Rev. C **86**, 015502 (2012).

[64] W. Haxton, Phys. Rev. D **36**, 2283 (1987).

[65] H. Minakata and H. Nunokawa, Phys. Rev. D **41**, 2976 (1990).

[66] Y.-Z. Qian and G. M. Fuller, Phys. Rev. D **49**, 1762 (1994).

[67] C. Lunardini and A. Y. Smirnov, Nucl. Phys. **B616**, 307 (2001).

[68] C. Lunardini and A. Y. Smirnov, J. Cosmol. Astropart. Phys. 06 (**2003**) 009.

[69] J. F. Beacom and L. E. Strigari, Phys. Rev. C **73**, 035807 (2006).

[70] S. Skadhauge and R. Zukanovich Funchal, J. Cosmol. Astropart. Phys. 04 (**2007**) 014.

[71] S. Skadhauge and R. Z. Funchal, arXiv:0802.1177.

[72] T. Akiri et al. (LBNE Collaboration), arXiv:1110.6249.

[73] J. F. Beacom and M. R. Vagins, Phys. Rev. Lett. **93**, 171101 (2004).

[74] M. Kachelrieß and R. Tomàs, Phys. Rev. D **71**, 063003 (2005).

[75] S. M. Adams, C. Kochanek, J. F. Beacom, M. R. Vagins, and K. Stanek, Astrophys. J. **778**, 164 (2013).

[76] M. T. Keil, G. G. Raffelt, and H.-T. Janka, Astrophys. J. **590**, 971 (2003).

[77] I. Tamborra, B. Muller, L. Hudepohl, H.-T. Janka, and G. Raffelt, Phys. Rev. D **86**, 125031 (2012).

[78] A. S. Dighe and A. Y. Smirnov, Phys. Rev. D **62**, 033007 (2000).

[79] A. Dighe, J. Phys. Conf. Ser. **136**, 022041 (2008).

[80] B. Dasgupta, A. Dighe, G. G. Raffelt, and A. Y. Smirnov, Phys. Rev. Lett. **103**, 051105 (2009).

[81] B. Dasgupta, Proc. Sci., ICHEP2010 (**2010**) 294.

[82] H. Duan, G. M. Fuller, and Y.-Z. Qian, Annu. Rev. Nucl. Part. Sci. **60**, 569 (2010).

[83] H. Duan, A. Friedland, G. C. McLaughlin, and R. Surman, J. Phys. G **38**, 035201 (2011).

[84] A. Friedland, Phys. Rev. Lett. **104**, 191102 (2010).

[85] Y. Pehlivan, A. Balantekin, T. Kajino, and T. Yoshida, Phys. Rev. D **84**, 065008 (2011).

[86] S. Sarikas, G. G. Raffelt, L. Hudepohl, and H.-T. Janka, Phys. Rev. Lett. **108**, 061101 (2012).

[87] J. F. Cherry, J. Carlson, A. Friedland, G. M. Fuller, and A. Vlasenko, Phys. Rev. Lett. **108**, 261104 (2012).

[88] A. S. Dighe, M. T. Keil, and G. G. Raffelt, J. Cosmol. Astropart. Phys. 06 (**2003**) 006.

[89] A. Dighe, M. Kachelriess, G. Raffelt, and R. Tomas, J. Cosmol. Astropart. Phys. 01 (**2004**) 004.

[90] J. F. Cherry, J. Carlson, A. Friedland, G. M. Fuller, and A. Vlasenko, Phys. Rev. D **87**, 085037 (2013).

[91] P. Vogel and J. Engel, Phys. Rev. D **39**, 3378 (1989).

[92] H. Zhang *et al.* (Super-Kamiokande Collaboration), arXiv:1311.3738.

[93] R. Tomas, D. Semikoz, G. Raffelt, M. Kachelriess, and A. Dighe, Phys. Rev. D **68**, 093013 (2003).

[94] K. Langanke, P. Vogel, and E. Kolbe, Phys. Rev. Lett. **76**, 2629 (1996).

[95] J. F. Beacom and P. Vogel, Phys. Rev. D **58**, 053010 (1998).

[96] J. F. Beacom and P. Vogel, Phys. Rev. D **58**, 093012 (1998).

[97] M. Ikeda *et al.* (Super-Kamiokande Collaboration), Astrophys. J. **669**, 519 (2007).

[98] K. Abe *et al.* (Super-Kamiokande Collaboration), Phys. Rev. D **83**, 052010 (2011).

[99] H. Watanabe, H. Zhang, K. Abe, Y. Hayato, T. Iida, M. Ikeda, J. Kameda, K. Kobayashi, Y. Koshio, and M. Miura (Super-Kamiokande Collaboration), Astropart. Phys. **31**, 320 (2009).

[100] M. R. Vagins, Nucl. Phys. B, Proc. Suppl. **229**–**232**, 325 (2012).

[101] J. F. Beacom and P. Vogel, Phys. Rev. D **60**, 033007 (1999).

[102] P. Antonioli *et al.*, New J. Phys. **6**, 114 (2004).

[103] T. Fischer, G. Martinez-Pinedo, M. Hempel, and M. Liebendorfer, Phys. Rev. D **85**, 083003 (2012).

[104] K. Nakazato, K. Sumiyoshi, H. Suzuki, T. Totani, H. Umeda, and S. Yamada, Astrophys. J. Suppl. Ser. **205**, 2 (2013).

[105] E. Kearns *et al.* (Hyper-Kamiokande Working Group Collaboration), arXiv:1309.0184.